THE JOURNAL OF PHYSICAL CHEMISTRY A LETTERS

2007, *111,* 2455−2457
Published on Web 03/14/2007

Reaction Force Decomposition of Activation Barriers To Elucidate Solvent Effects

Jaroslav V. Burda,[†] Alejandro Toro-Labbé,*,[‡] Soledad Gutiérrez-Oliva,[‡] Jane S. Murray,[§] and Peter Politzer*,[§,#]

Department of Chemical Physics and Optics, Faculty of Mathematics and Physics, Charles University, Ke Karlovu 3, 112 16 Prague, Czech Republic, Laboratorio de Química Teórica Computacional (QTC), Facultad de Química, Pontificia Universidad Católica de Chile, Vicuña Mackenna 4860, Casilla 306, Correo 22, Santiago, Chile, Department of Chemistry, Cleveland State University, Cleveland, Ohio 44115, and Department of Chemistry, University of New Orleans, New Orleans, Louisiana 70148

Received: February 2, 2007; In Final Form: February 19, 2007

The reaction force $\mathbf{F}(\mathbf{R}_c)$ of a chemical or physical process is given by the negative derivative of the potential energy $V(\mathbf{R}_c)$ along the intrinsic reaction coordinate $\mathbf{R}_c$. $\mathbf{F}(\mathbf{R}_c)$ unambiguously and naturally divides the activation barrier in each direction into two contributions, one of which has been found to reflect preparative structural factors, $E_{act,prep}$, and the other corresponds to the first part of the transition to products, $E_{act,trans}$. We have analyzed $\mathbf{F}(\mathbf{R}_c)$ for an S_N2 substitution reaction in both the gas and aqueous phases. Although the overall forward and reverse activation barriers are significantly lowered by the solvent, the $E_{act,trans}$ are very little affected. Thus the increased rates that are predicted for this process in aqueous solution can be attributed to the solvent facilitating the structural effects in the preparative stages, decreasing the $E_{act,prep}$. This example shows how the reaction force decomposition of activation barriers can help to elucidate the roles played by external factors, e.g., solvents.

With any chemical or physical process, there is associated a "reaction force" $\mathbf{F}(\mathbf{R}_c)$, given by

$$\mathbf{F}(\mathbf{R}_c) = -\frac{\partial V(\mathbf{R}_c)}{\partial \mathbf{R}_c} \tag{1}$$

where $V(\mathbf{R}_c)$ is the potential energy of the system along the intrinsic reaction coordinate $\mathbf{R}_c$. For a process having an activation barrier in both the forward and reverse directions, as in Figure 1, the $\mathbf{F}(\mathbf{R}_c)$ profile has the characteristic form shown, with a minimum and a maximum at the inflection points of $V(\mathbf{R}_c)$. This profile identifies three key points in the process: the minimum and maximum of $\mathbf{F}(\mathbf{R}_c)$ at $R_c = \alpha$ and γ, and the transition state at $R_c = \beta$, where $\mathbf{F}(\mathbf{R}_c) = 0$.

The points $R_c = \alpha$, β, and γ define four zones along $\mathbf{R}_c$. In a series of studies,[1−8] we have found that certain generalizations can be made about what occurs in each of these zones. In the first, between the reactants and $R_c = \alpha$, the emphasis tends to be upon preparative structural effects that will facilitate subsequent steps, e.g., bond stretching, rotations, etc. In this zone, electronic properties, such as ionization energies, usually change only slowly and gradually.

The second and third zones, from $R_c = \alpha$ to β to γ, can be viewed as "transition to products." This features new bonds forming (if the process is a chemical reaction). Although structural effects continue, what is strikingly distinctive about these zones are the rapid and extensive variations in electronic properties. (Examples will be shown later in this paper.) After $R_c = \gamma$, the emphasis is upon structural relaxation to the final products, although some bond formation/breaking might still take place. An analogous description applies to the reverse process, for which $\mathbf{F}(\mathbf{R}_c)$ is the negative of that in Figure 1, due to $\mathbf{R}_c$ having the opposite direction.

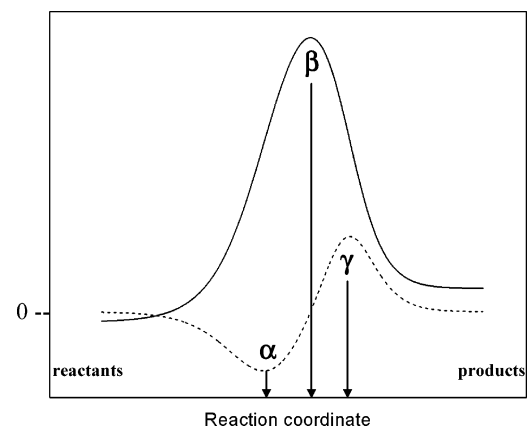

Figure 1. Characteristic profiles along the intrinsic reaction coordinate $\mathbf{R}_c$ of the potential energy $V(\mathbf{R}_c)$ and the reaction force $\mathbf{F}(\mathbf{R}_c)$, for a process having an activation barrier in both directions. $V(\mathbf{R}_c)$ and $\mathbf{F}(\mathbf{R}_c)$ are shown in solid and dashed lines, respectively. The zero of $\mathbf{F}(\mathbf{R}_c)$ is indicated. The points $R_c = \alpha$ and $R_c = \gamma$ correspond to the minimum and maximum of $\mathbf{F}(\mathbf{R}_c)$; the transition state is at $R_c = \beta$.

* Corresponding authors. P.P. e-mail: ppolitze@uno.edu. A.T.-L. e-mail: atola@uc.cl.
[†] Charles University.
[‡] Pontificia Universidad Católica de Chile.
[§] Cleveland State University.
[#] University of New Orleans.

10.1021/jp0709353 CCC: $37.00 © 2007 American Chemical Society

The key point brought out by Figure 1, in terms of our present objective, is that the activation barrier in each direction has two components. For the forward direction,

$$E^{\mathrm{f}}_{\mathrm{act}} = -\int_{\substack{\mathrm{reactants}\\ \mathrm{minimum}}}^{R_c=\alpha} \mathbf{F}(\mathbf{R}_c)\cdot \mathrm{d}\mathbf{R}_c - \int_{R_c=\alpha}^{R_c=\beta} \mathbf{F}(\mathbf{R}_c)\cdot \mathrm{d}\mathbf{R}_c = E^{\mathrm{f}}_{\mathrm{act,prep}} + E^{\mathrm{f}}_{\mathrm{act,trans}} \quad (2)$$

The two contributions to $E^{\mathrm{f}}_{\mathrm{act}}$ represent the energies required for the initial preparative phase of the process, $E^{\mathrm{f}}_{\mathrm{act,prep}}$, and the first part of the transition to products, $E^{\mathrm{f}}_{\mathrm{act,trans}}$. Decomposition of the activation barrier into its two components can provide insight into the mechanism of a process and into the roles of external factors that may influence its rate, such as solvents and catalysts. Our purpose in this paper is to show how $\mathbf{F}(\mathbf{R}_c)$ and eq 2 can help to elucidate the role of a solvent.

We have recently applied the reaction force concept to analyzing, with the B3LYP/6-31G* procedure, the gas-phase S_N2 substitution[7]

$$H_3C{-}Cl + H{-}OH \rightarrow H_3C{-}OH + H{-}Cl \quad (3)$$

We have now repeated this at the CCSD(T)/aug-cc-pVTZ level and examined also the effect of a solvent, using a conductor-like screening model (COSMO) continuum approach,[9,10] as implemented in the Gaussian 03 code.[11] The dielectric constant was 78.39, taken from the COSMO database; this is very similar to the value for water at 20 °C, 80.10.[12] It corresponds, therefore, to a highly polar solvent. All ΔE values to be presented will be from energy minima at 0 K.

Both the reactants and the products in reaction 3 interact with each other via hydrogen bonds, $H_3C{-}Cl$---$H{-}OH$ in the former and $H_3C{-}(H)O$---$H{-}Cl$ in the latter. In the gas phase, these complexes are respectively 4.0 and 6.6 kcal/mol lower in energy than the separated reactants and products. In solution, the values are 1.1 and 4.8 kcal/mol. Our CCSD(T) $V(\mathbf{R}_c)$ and $\mathbf{F}(\mathbf{R}_c)$ profiles for this reaction, presented in Figure 2, begin at the reactant complex and terminate at the product complex.

As discussed earlier,[7] in the gas phase, the major event in the preparative zone of reaction 3, prior to the $\mathbf{F}(\mathbf{R}_c)$ minimum at $R_c = \alpha$, is the stretching of the C−Cl bond by about 0.5 Å, with the Cl becoming more negative; this is accompanied by the CH_3 group becoming more planar and the H_2O moving toward it. In proceeding from $R_c = \alpha$ to the transition state at $R_c = \beta$, the C−O bond begins to form, while the Cl continues to move away from the carbon and increasingly acquires Cl^- character. At the transition state, the H_2O molecule is still largely intact. Between $R_c = \beta$ and $R_c = \gamma$, however, the HO−H bond stretches by nearly 0.2 A, and the Cl---H becomes more covalent. The final separation of H from OH and the relaxation of the Cl−H and C−O bonds to their values in the product complex is after $R_c = \gamma$.

The sequence of steps is qualitatively similar in the solution, but the Cl moves away from the CH_3 more rapidly and the H_2O remains essentially intact longer. The polar solvent presumably promotes the departure of the quasi-Cl^- ion, $Cl^{\delta-}$.

In Figure 3, we have plotted the variations of two electronic properties along $\mathbf{R}_c$: the energy of the highest occupied molecular orbital and the hardness, η. The latter was estimated from the highest-occupied and lowest-unoccupied molecular orbital energies, ϵ_{HOMO} and ϵ_{LUMO}, by the widely used approximation $\eta \approx \epsilon_{\mathrm{LUMO}} - \epsilon_{\mathrm{HOMO}}$.[13,14] Figure 3 illustrates our earlier statement that the greatest changes in electronic properties, in both the gaseous and the aqueous phases, occur between

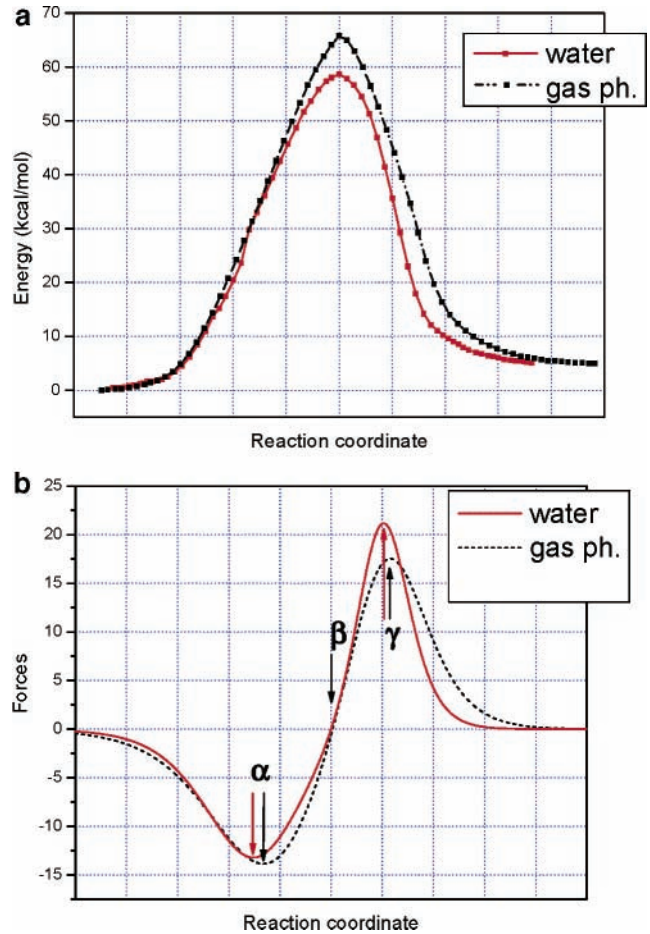

Figure 2. Profiles of (a) the potential energy $V(\mathbf{R}_c)$ and (b) the reaction force $\mathbf{F}(\mathbf{R}_c)$, along the intrinsic reaction coordinate $\mathbf{R}_c$ for the reaction in eq 3, in the gas phase and in aqueous solution. The points $R_c = \alpha$, β, and γ indicate respectively the minimum of $\mathbf{F}(\mathbf{R}_c)$, the transition state, and the maximum of $\mathbf{F}(\mathbf{R}_c)$. In the gas phase, $\alpha = -2.65$, $\beta = 0.0$, and $\gamma = 2.32$; in the solution, $\alpha = -3.05$, $\beta = 0.0$, and $\gamma = 2.06$. The reactant and product complexes are at −10.0 and +10.0. The units of $\mathbf{F}(\mathbf{R}_c)$ are those corresponding to $V(\mathbf{R}_c)$ in kcal/mol.

$R_c = \alpha$ and $R_c = \gamma$; both the HOMO energy and the hardness pass through extrema between these points.

The overall gas phase ΔE for the forward process in eq 3, from separate reactants to separate products, is 7.6 kcal/mol. With B3LYP/6-31G* vibrational and thermal corrections, this yields $\Delta H(298\ \mathrm{K}) = 6.8$ kcal/mol, in good agreement with the experimental 7.7 kcal/mol from gas phase heats of formation.[15] The predicted ΔE in aqueous solution is 9.1 kcal/mol.

Figure 2a shows that aqueous solution has the effect of lowering the activation barriers. For the forward process, the change is 7.8 kcal/mol (from 66.6 to 58.8) and for the reverse, 8.3 kcal/mol (from 61.6 to 53.3). (The activation barriers are calculated relative to the reactant and product complexes.)

The energetic results presented up to this point have come entirely from $V(\mathbf{R}_c)$. What additional insight can $\mathbf{F}(\mathbf{R}_c)$ provide? In Table 1 are given the values of the components of the forward and reverse activation barriers, as defined by the reaction force, Figure 2b and eq 2. Note that for the reverse process, $\mathbf{F}(\mathbf{R}_c)$ would be the negative of that shown; the preparative zone would be from the complex to $R_c = \gamma$, and the first transition zone from $R_c = \gamma$ to $R_c = \beta$.

The striking feature of the data in Table 1, in the context of our present objective, is that both $E^{\mathrm{f}}_{\mathrm{act,trans}}$ and $E^{\mathrm{r}}_{\mathrm{act,trans}}$ are very similar in the gaseous and the aqueous phases, even though the points $R_c = \alpha$ and $R_c = \gamma$ have shifted slightly relative to the

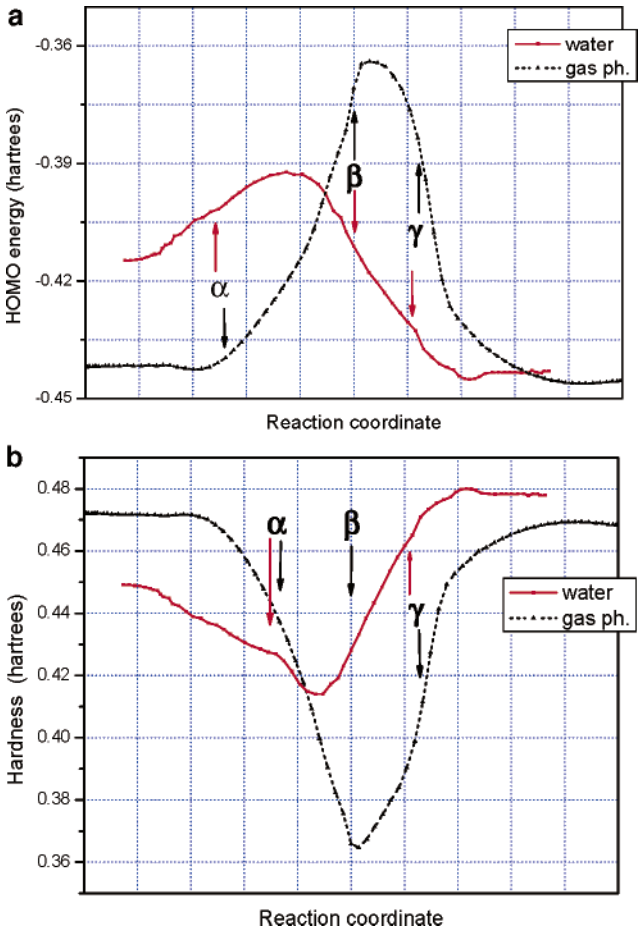

Figure 3. Variation of (a) the energy of the highest-occupied molecular orbital and (b) the hardness, along the intrinsic reaction coordinate $\mathbf{R}_c$ for the reaction in eq 3, in the gas phase, and in aqueous solution. The points $R_c = \alpha$, β, and γ correspond respectively to the minimum of $\mathbf{F}(\mathbf{R}_c)$, the transition state, and the maximum of $\mathbf{F}(\mathbf{R}_c)$. In the gas phase, $\alpha = -2.65$, $\beta = 0.0$, and $\gamma = 2.32$; in the solution, $\alpha = -3.05$, $\beta = 0.0$, and $\gamma = 2.06$. The reactant and product complexes are at -10.0 and $+10.0$.

TABLE 1: Computed Components of the Forward and Reverse Activation Barriers of the Reaction in Eq 3[a]

component	zone	gas phase[b]	aqueous[b]
	Forward Reaction		
$E^{f}_{act,prep}$	preparative; complex $\rightarrow R_c = \alpha$	39.1	32.6
$E^{f}_{act,trans}$	transition; $R_c = \alpha \rightarrow R_c = \beta$	27.5	26.2
	Reverse Reaction		
$E^{r}_{act,prep}$	preparative; complex $\rightarrow R_c = \gamma$	34.9	29.1
$E^{r}_{act,trans}$	transition; $R_c = \gamma \rightarrow R_c = \beta$	26.7	24.2

[a] CCSD(T)/aug-cc-pVTZ calculations. [b] Units are kcal/mol.

transition state (Figure 2b). Thus the energy required for the first part of the transition to products, which is where covalent bond formation and/or breaking primarily start to occur, is very little affected (1−2 kcal/mol) by the presence of the solvent, for both the forward and reverse reactions. It is in the preparative zones that the solvent's influence is most felt (∼6 kcal/mol). In the forward process, it helps the negative Cl move away from the CH_3 group, which is reflected in Figure 3a by the shifting of the HOMO energy maximum in solution to earlier in the reaction; the HOMO is associated largely with the $Cl^{\delta-}$. In the reverse process, the solvent assists an $H^{\delta+}$ to leave the $Cl^{\delta-}$.

From the $V(\mathbf{R}_c)$ profiles in Figure 2a, it might well be concluded that the lowering of the activation barriers by the solvent is due to its stabilizing the transition state relative to the reactant and product complexes. The solvent is certainly interacting with the system throughout the course of the reaction; this presumably accounts for the 1−2 kcal/mol decreases in $E^{f}_{act,trans}$ and $E^{r}_{act,trans}$ that do take place. However, decomposing the activation barriers into their components in accordance with $\mathbf{F}(\mathbf{R}_c)$ indicates that the main effects of the solvent are localized in the preparative stages, facilitating the structural changes that occur there.

The conclusions that have been reached in this work are of course specific to the reaction in eq 3. What it has demonstrated, however, is that reaction force analysis provides a rational and unambiguous basis for decomposing activation barriers into contributions that help to explain how external influences, e.g., solvents, affect reaction rates.

Acknowledgment. We greatly appreciate the suggestion of Dr. Benedetta Mennucci that the effects of solvents upon the reaction force be investigated. We are grateful for support provided to J.V.B. by the MŠMT ČR grant project MSM 0021620835 and to A.T.-L. by the Proyecto FONDECYT #1060590, the Proyecto FONDAP #11980002 (CIMAT), the Proyecto PBCT de Inserción Academica, and a fellowship from the John Simon Guggenheim Foundation. S.G.-O. acknowledges financial support from Núcleo Milenio de Mecánica Cuántica Aplicada y Química Computacional, Código P02-004-F.

References and Notes

(1) Jaque, P.; Toro-Labbé, A. *J. Phys. Chem. A* **2000**, *104*, 995.
(2) Toro-Labbé, A.; Gutiérrez-Oliva, S.; Concha, M. C.; Murray, J. S.; Politzer, P. *J. Chem. Phys.* **2004**, *121*, 4570.
(3) Herrera, B.; Toro-Labbé, A. *J. Chem. Phys.* **2004**, *121*, 7096.
(4) Martinez, J.; Toro-Labbé, A. *Chem. Phys. Lett.* **2004**, *392*, 132.
(5) Gutiérrez-Oliva, S.; Herrera, B.; Toro-Labbé, A.; Chermette, H. *J. Phys. Chem. A* **2005**, *109*, 1748.
(6) Politzer, P.; Toro-Labbé, A.; Gutiérrez-Oliva, S.; Herrera, B.; Jaque, P.; Concha, M. C.; Murray, J. S. *J. Chem. Sci.* **2006**, *117*, 467.
(7) Politzer, P.; Burda, J. V.; Concha, M. C.; Lane, P.; Murray, J. S. *J. Phys. Chem. A* **2006**, *110*, 756.
(8) Gutiérrez-Oliva, S. *J. Phys. Chem. A*, submitted for publication.
(9) Klamt, A.; Schüürmann, G. *J. Chem. Soc., Perkin Trans. 2* **1993**, 799.
(10) Klamt, A. *J. Phys. Chem.* **1995**, *99*, 2224.
(11) Frisch, M. J; Trucks, G. W.; Schlegel, H. B.; Scuseria, G. E.; Robb, M. A.; Cheeseman, J. R.; Montgomery, J. A., Jr.; Vreven, T.; Kudin, K. N.; Burant, J. C.; Millam, J. M.; Iyengar, S. S.; Tomasi, J.; Barone, Mennucci, V. B.; Cossi, M.; Scalmani, G.; Rega, N.; Petersson, G. A.; Nakatsuji, H.; Hada, M.; Ehara, M.; Toyota, K.; Fukuda, R.; Hasegawa, J.; Ishida, M.; Nakajima, T.; Honda, Y.; Kitao, O.; Nakai, H.; Klene, M.; Li, X.; Knox, J. E.; Hratchian, H. P.; Cross, J. B.; Adamo, C.; Jaramillo, J.; Gomperts, R.; Stratmann, R. E.; Yazyev, O.; Austin, A. J.; Cammi, R.; Pomelli, C.; Ochterski, J. W.; Ayala, P. Y.; Morokuma, K.; Voth, G. A.; Salvador, P.; Dannenberg, J. J.; Zakrzewski, V. G.; Dapprich, S.; Daniels, A. D.; Strain, M. C.; Farkas, O.; Malick, D. K.; Rabuck, A. D.; Raghavachari, K.; Foresman, J. B.; Ortiz, J. V.; Cui, Q.; Baboul, A. G.; Clifford, S.; Cioslowski, J.; Stefanov, B. B.; Liu, G.; Liashenko, A.; Piskorz, P.; Komaromi, I.; Martin, R. L.; Fox, D. J.; Keith, T.; Al-Laham, M. A.; Peng, C. Y.; Nanayakkara, A.; Challacombe, M.; Gill, P. M. W.; Johnson, B.; Chen, W.; Wong, M. W.; Gonzalez, C.; Pople, J. A. *Gaussian 03*, revision C.02; Gaussian, Inc.: Wallingford, CT, 2004.
(12) Lide, D. R., Ed. *Handbook of Chemistry and Physics*, 85th ed.; CRC Press: New York, 2004.
(13) Parr, R. G.; Yang, W. *Density-Functional Theory of Atoms and Molecules*; Oxford University Press: New York, 1989.
(14) Morell, C.; Grand, A.; Toro-Labbé, A. *J. Phys. Chem. A* **2005**, *109*, 205.
(15) Mallard, W. G., Linstrom, P. J., Eds. *NIST Chemistry Webbook*; NIST Standard Reference Database No. 69; NIST: Gaithersburg, MD, 1998; http://webbook.nist.gov.